ELSEVIER

Biochimica et Biophysica Acta 1467 (2000) 39–53

BIOCHIMICA ET BIOPHYSICA ACTA

BBA

www.elsevier.com/locate/bba

Interactions between cholesterol and lipids in bilayer membranes. Role of lipid headgroup and hydrocarbon chain–backbone linkage

Santanu Bhattacharya [a,b,*], Saubhik Haldar [a]

[a] *Department of Organic Chemistry, Indian Institute of Science, Bangalore 560 012, India*

[b] *Chemical Biology Unit, Jawaharlal Nehru Centre for Advanced Scientific Research, Bangalore 560 012, India*

Received 13 December 1999; received in revised form 14 March 2000; accepted 17 March 2000

Abstract

We have employed four lipids in the present study, of which two are cationic and two bear phosphatidylcholine (PC) headgroups. Unlike dipalmitoylphosphatidylcholine, the other lipids employed herein do not have any ester linkage between the hydrocarbon chains and the respective lipid backbones. Small unilamellar vesicles formed from each of the PC and cationic lipids with or without varying amounts of cholesterol have been examined using the steady-state fluorescence anisotropy method as a function of temperature. The anisotropy data clearly indicate that the order in the lipid bilayer packing is strongly affected upon inclusion of cholesterol. This effect is similar irrespective of the electrostatic character of the lipid employed. The influence of cholesterol inclusion on multi-lamellar lipid dispersions has also been examined by ^{1}H-nuclear magnetic resonance spectroscopy above the phase transition temperatures. With all the lipids, the line widths of $(CH_2)_n$ protons of hydrocarbon chains in the NMR spectra respond to the addition of cholesterol to membranes. The influence on the bilayer widths of various lipids upon inclusion of cholesterol was determined from X-ray diffraction studies of the cast films of the lipid–cholesterol coaggregates in water. The effect of cholesterol on the efflux rates of entrapped carboxyfluorescein (CF) from the phospholipid vesicles was determined. Upon incremental incorporation of cholesterol into the phospholipid vesicles, the CF leakage rates were progressively reduced. Independent experiments measuring trans-membrane OH^- ion permeation rates from cholesterol-doped cationic lipid vesicles using entrapped dye riboflavin also demonstrated that the addition of cholesterol into the cationic lipid vesicles reduced the leakage rates irrespective of lipid molecular structure. It was found that the cholesterol induced changes on the membrane properties such as lipid order, linewidth broadening, efflux rates, bilayer widths, etc., did not depend on the ability of the lipids to participate in the hydrogen bonding interactions with the 3β-OH of cholesterol. These findings emphasize the importance of hydrophobic interaction between lipid and cholesterol and demonstrate that it is not necessary to explain the observed cholesterol induced effects on the basis of the presence of hydrogen bonding between the 3β-OH of cholesterol and the lipid chain–backbone linkage region or headgroup region.

Keywords: Lipid–cholesterol interaction; Chain–backbone linkage; Lipid headgroup; Cationic lipid; Phospholipid

1. Introduction

In erythrocyte and myelin membranes cholesterol constitutes up to 40% of the total lipid [1]. Mammalian cells require cholesterol for normal cell function

* Corresponding author. Fax: +91-80-334-1683; E-mail: sb@orgchem.iisc.ernet.in

0005-2736/00/$ – see front matter
PII: S0005-2736(00)00196-6

and this requirement can be fulfilled by endogenous biosynthesis of the sterol or by extracellular supplements and in general both mechanisms are used [2]. One of the primary roles of cholesterol in eukaryotic cells is to modulate the physical properties of the plasma membrane phospholipid bilayer [3]. Incorporation of cholesterol in both model and intact membranes induces diverse changes in the bilayer properties. For example, this reduces molecular surface area [4–6] and membrane permeabilities [7,8], alters lateral diffusion rates for both proteins and lipids [9,10], broadens gel to liquid-crystalline phase transition and moderates acyl chain order in both the gel and liquid-crystalline phases [11]. Rotational diffusion studies incorporating androstane spin label (ASL), a sterol analog, suggest that cholesterol decreases both the cone angle and the wobbling rotational diffusion constant for ASL in both saturated and unsaturated phosphatidylcholine (PC) membranes [12]. A number of studies involving electron spin resonance (ESR) [13,14], Raman [15,16], Fourier transform infrared (FT-IR) [17] and ^{2}H-nuclear magnetic resonance (NMR) [18] methods led to a conception that cholesterol fluidizes and/or induces disorders in the phospholipid organization in membrane below the gel–liquid-crystalline phase transition temperature T_m, while rigidifying at temperatures above T_m.

Earlier studies suggested that a hydrogen bond exists between the hydroxyl group of cholesterol and the phosphate headgroup of phospholipid [19]. However, the presence of such a hydrogen bond was refuted by subsequent ^{13}C-NMR and ^{31}P-NMR studies [20]. Another possible site of hydrogen bonding with 3β-OH of cholesterol is the ester carbonyl bond of the diacyl PC lipids. The X-ray and neutron diffraction data showed that the 3β-OH group of cholesterol is aligned with the ester carbonyl groups of PC lipids at the hydrocarbon–water interface of PC/cholesterol mixed bilayers, [21,22] suggesting the existence of (PC)–C=O.....H-O–(cholesterol) type interactions. However, independent studies using Raman [23], infrared spectroscopy [24] or studies of membrane permeability [25] with PC membrane in the presence or absence of cholesterol found no evidence of hydrogen bonding between cholesterol and the carbonyl groups at the diester linkages of the PC lipids. This type of hydrogen bond formation was also addressed by Demel et al. where cholesteryl ether was used to prevent the hydrogen bond formation with lipid [26]. Therefore, the molecular basis of cholesterol–lipid association, has not been unequivocally established ([27] and references therein).

Previous efforts in this laboratory were directed toward the design and synthesis of new membrane-forming amphiphiles [28–30] and studies of their aggregation behavior. We have also studied the interaction of various natural components of membranes with selected lipid aggregates [31,32]. In the present study we decided to examine the nature of cholesterol association with lipids in membrane, by selecting two types of lipids. One type comprises of two cationic lipids (**1**, **2**) which are devoid of any functional group at the linkage with the hydrocarbon chains and the lipid backbone. As a consequence, these lipids cannot participate in the hydrogen bonding with the 3β-OH of cholesterol either at the headgroup or at chain–backbone links. The second type of lipids (**3**, **4**) on the other hand are phospholipids with zwitterionic PC residues as headgroups. However, **3** and **4** differ in that their hydrocarbon chains are connected with the lipid backbone. Thus while **4** is a PC lipid with natural ester links with both the hydrocarbon chains, in **3**, the hydrocarbon chains are non-scissile and are part of the lipid backbone.

From a biophysical perspective, the present study is of interest as this addresses the comparisons of the nature of interaction of cholesterol with cationic lipid aggregates against natural zwitterionic lipids with a PC headgroup. Furthermore the synthetic availability of the lipids with selected structural features allows investigation of the role of chain–backbone links in this interaction. In this paper we present the results of cholesterol interaction with membranes of each of these lipids by measuring fluorescence depolarization and excitation lifetime of the probe 1,6-diphenyl-1,3,5-hexatriene (DPH)-doped in these coaggregates. ^{1}H-NMR studies have been performed to examine the influence of cholesterol incorporation on the $(CH_2)_n$ proton linewidths of hydrophobic chains of different lipid aggregates above their phase transition temperature. We also investigate the role of the chain–backbone linkage in PC lipids on the permeation rates of entrapped 5/6-carboxyfluorescein (CF) as a function of cholesterol concentration. Cholesterol appears to alter bilayer thicknesses as revealed from X-ray diffraction studies. These studies

clearly establish that cholesterol induced changes in lipid order, reduction in permeation rates or alteration in bilayer widths takes place irrespective of the nature of the chain–backbone linkages.

2. Materials and methods

All the reagents and chemicals used in this study are of the highest purity (ACS grade) available. The lipids used in this present study have been synthesized according to a procedure described elsewhere [33] and the ^{1}H-NMR, IR, mass spectral and elemental analyses data for the newly synthesized lipids were consistent with their given structures.

2.1. Unilamellar vesicle preparation

Separate solutions of different lipids in the presence or in the absence of cholesterol in chloroform were evaporated to dryness in Wheaton vials under a stream of dry nitrogen gas and then under high vacuum to prepare thin films of the lipids on the walls of the vials. Either the film of the dried lipid or the lipid/cholesterol mixture was dispersed in water (Millipore) and the resulting suspension was left for hydration for ca. 1 h at 4°C. The suspension was then thawed to 65°C for 10 min and cooled to 4°C for 15 min. The freeze–thaw cycles were repeated 2–3 times to ensure optimal hydration. The lipid or lipid–cholesterol suspensions thus obtained were sonicated individually above their thermotropic phase transition temperature using a bath type sonicator for 15 min to give small unilamellar vesicles (SUVs).

2.2. Fluorescence anisotropy measurements

The fluorescence emission spectrum was recorded by excitation of membrane-doped DPH at 360 nm. The maximum peak height of the emission was recorded at 430 ± 3 nm. The slit widths of both the excitation and emission window were kept at 5 nm. The fluorescence intensity of the emitted light polarized parallel ($I_{\parallel}$) and perpendicular ($I_{\perp}$) to the excited light was recorded with temperature. These fluorescence intensities were corrected for the scattered light intensity, which was determined independently for an unlabeled reference suspension by the identical procedure. There was no polarization due to light scattering, since the dilution of DPH-doped vesicles had no effect on the fluorescence polarization. The fluorescence polarization, P, was calculated according to $P=(I_{\parallel}-GI_{\perp})/(I_{\parallel}+GI_{\perp})$, where G is the instrumental grating factor. The corresponding anisotropies (r) were measured by employing the Perrin equation, $r=(I_{\parallel}-GI_{\perp})/(I_{\parallel}+2GI_{\perp})$.

The apparent gel-to-liquid-crystalline phase transition temperatures were calculated from the midpoints of the breaks related to the temperature-dependent r values [34–36]. The temperature range for phase transition was calculated from the two temperature points for each experiments which marked the beginning and the end of the phase transition process. The fluorescence anisotropies due to DPH-doped in different lipid–cholesterol mixtures were also measured. Following the reported procedure of Pottel et al. [37] the microviscosities of the cholesterol-doped lipid membranes were then determined.

2.3. ^{1}H-NMR Studies

^{1}H-NMR experiments with various cholesterol-free and doped lipid vesicles were conducted according to a published procedure [28].

2.4. Emission lifetime measurements of DPH in medium-sized lamellar vesicles (MLVs)

Decays of the fluorescence intensity of DPH incorporated in various vesicular systems were measured by the single photon counting method using an IBH-500 SPC instrument. A hydrogen discharge lamp operated at a pressure of 0.5 bar was used as light source. The excitation wavelength was 360 nm whereas the emission was monitored at 430 nm keeping the bandwidths at 12 nm. The data were collected in 1024 channels using a multi-channel analyzer. In each experiment 1000 peak counts were acquired. A lamp profile was collected for each sample decay curve using a standard MgO suspension in water as the scattering solution. The decay time in each vesicle preparation was measured at 25°C.

The decay of fluorescence intensity is represented as a sum of the multi-exponential such as $I(t)=I_0\sum_i e^{-t/\tau_i}$, which was analyzed by a non-linear least square deconvolution procedure. The good-

ness of the fit was judged by the standard statistical test, i.e. random distribution of weighted residuals, the auto correlation function and the values of χ^2 and residuals. The fractional intensity (f_i) is given by: $f_i = \alpha_i\tau_i/\Sigma\alpha_i\tau_i$, where α is the pre-exponential factor and τ is the decay time. Each reported lifetime value is the mean of three to four independent determinations.

2.5. Entrapment of 5/6-CF and fluorescence assay of its release

The entrapment of 5/6-CF in vesicles and its subsequent release was carried out following a reported procedure [38,39]. Briefly, 2.5 mM suspensions (SUV) of DHPPC-doped with different percentages of cholesterol were prepared in Tris–HCl buffer (50 mM, pH 8.3) containing 50 mM of CF upon dispersion of the lipid suspensions in a bath type sonicator for 15 min. The liposomes loaded with CF were separated from the free dye by passing through a Sephadex G-50 column with an elution buffer of 50 mM Tris–HCl, 50 mM Na_3PO_4, pH 8.3. Several aliquots of the eluted fractions were collected and stored under an ice-jacket. An aliquot (100 μl) of one of the most CF intense fractions was taken and diluted to 2.9 ml with elution buffer and the transmembrane permeation was measured at 25°C by following the changes in emission due to CF as a function of time. The excitation and emission wavelengths used for this experiment were 495 and 520 nm, respectively. Percentage CF releases were measured with respect to the total fluorescence intensity (F_f) obtained after disrupting the vesicular aggregate with 10% (w/v) Triton X-100 (final concentration: 0.15% w/v) and by following the equation: % release $= [(F_t - F_i)/(F_f - F_i)] \times 100$, where F_i, F_t and F_f are the fluorescence emission values at time $t = 0$, at time t and the final fluorescence on disruption of the vesicles, respectively. Time-dependent changes of the fluorescence emission from a few individual determinations for a given lipid or lipid–cholesterol blends were averaged and followed a single exponential path.

2.6. Riboflavin entrapment in cationic lipid vesicles and trans-membrane permeation assay

The entrapment of a neutral dye, riboflavin, in cationic lipid vesicles of DODAB, **1** and DOETAB, **2** was performed following a published procedure [40]. Briefly, individual suspensions of DODAB or DOETAB (2 mM) containing different amounts of cholesterol were prepared in aqueous solution (pH ~ 6.4) of riboflavin (0.2 mM) by reverse evaporation. Each of the resulting suspensions was loaded onto a Sephadex G-50 column and then gel-filtered to separate the vesicles loaded with riboflavin from the free dye. Several aliquots of the eluted fractions were collected and stored under an ice-jacket.

2.7. X-ray diffraction measurement of cast bilayer films

Different vesicular suspensions of the lipids (10 mg/ml) in the presence or absence of different mol% of cholesterol were cast on separate glass slides to form thin films, which were air-dried at ambient temperature. Each of these samples was examined by the X-ray diffraction method as described [41,42] using a Seifert model X-ray diffractometer. The wavelength of the monochromatized Cu-K_α beam was 1.540598 Å and it was directed toward the film edge and the scanning was performed up to a 2θ value of 20°.

2.8. Calculation of molecular lengths of the lipids

The energy minimized, preferred conformations of all the lipids were computed using the INSIGHT II molecular simulation program (DISCOVER) following a published procedure. [40]

3. Results and discussion

Examination of the molecular structures of various naturally occurring lipids reveals that although all lipid molecules are amphiphilic in character important differences exist in their architectures. These differences are obvious at the headgroup region or with the hydrocarbon chains that vary either in length or in the degree of unsaturation. However, a more subtle yet crucial difference exists in lipid structures, in which the functional groups at the lipid backbone that connects hydrocarbon chains with the polar

headgroup vary. Thus, while most glycerophospholipids bear *ester* type of connections between its fatty acyl chains and the glycerol backbone, in sphingomyelin it is an *amide* group that serves as the link between the hydrocarbon chain and the sphingosine lipid backbone of the lipid [43]. On the other hand, the phospholipids with alkyl and alk-1-enyl *ether* linkages occur in eukaryotic cell membranes of both normal healthy cells and more frequently in malignant cancer cells [44,45]. Earlier studies with model and reconstituted ether and ester derived phospholipid vesicles showed significant differences in their diffusion properties and in their intermolecular interactions with other membrane constituents [46]. Such differences in the chain–backbone links suggest a role of the connector functional units in the modulation of mutual intra- and inter-monomer interactions within the membranes and their association with other molecules.

The importance of the presence of hydrogen bonding at the chain linkage functional groups or at the level of lipid headgroups also becomes obvious in explaining the inter-lipid interactions in membranes. However, there is no consensus about the specific details of interaction that exists between cholesterol and phospholipid molecules in the membranes. Since the preceding studies hypothesize the role of both the headgroup and the chain-linkage functional groups of lipids in its association with cholesterol via hydrogen bonding through its 3β-OH group, we thought it imperative to investigate this issue with two types of lipids.

3.1. Choice of lipids

We have selected two types of lipids for the examination of the nature of the cholesterol–lipid interactions in membranes (Scheme 1). First we have taken two cationic lipids, DODAB, **1**, and DOETAB, **2**, which are devoid of any functional group at the linkages with the lipid backbone and the hydrocarbon chains. Thus, neither of these two lipids can participate in hydrogen bonding type interactions with the 3β-OH of cholesterol either at the headgroup level or at the linkage region between the hydrocarbon chains and the lipid backbone. Although cationic, **1** and **2** differ in terms of their architecture. **1** is a well-known lipid used in membrane related studies for nearly two decades. The hydrocarbon chains in **1** are geminally anchored in a symmetric fashion to the NMe_2^+ headgroup. However, **2** is new, where the hydrocarbon chains are separated from the $-NMe_3^+$ headgroup by one CH_2 unit. The two octadecyl chains in **2** are attached at the 2-position of an ethyl group while the 1-position in **2** is occupied by the trimethylammonium functionality. Thus the molecular structure in **2** resembles the *vicinal* disposition of acyl hydrocarbon chains at the C-1 and C-2 positions of the glycerol backbone in dipalmitoylphosphatidylcholine (DPPC) (**4**), although the phospho-

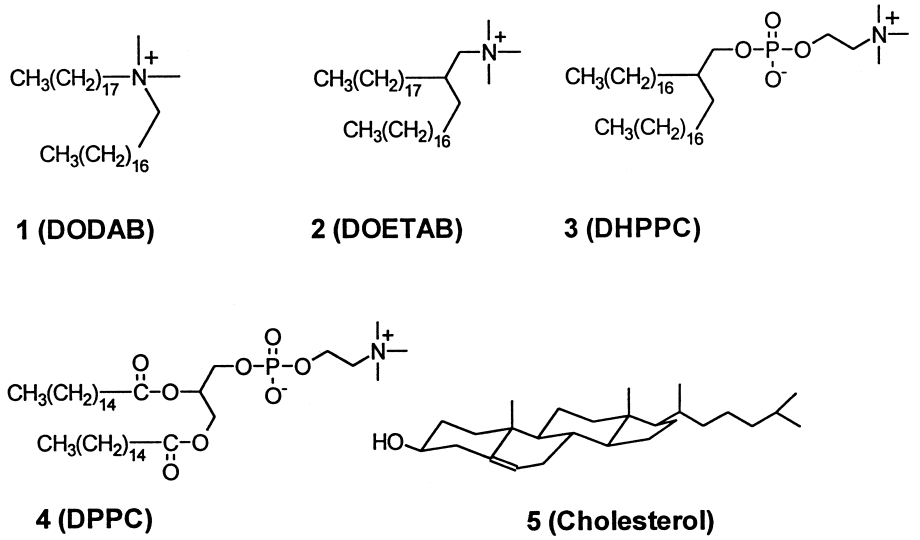

Scheme 1. The structure of the lipids used for present studies. (**1**) DODAB, (**2**) DOETAB, (**3**) DHPPC, (**4**) DPPC and (**5**) cholesterol.

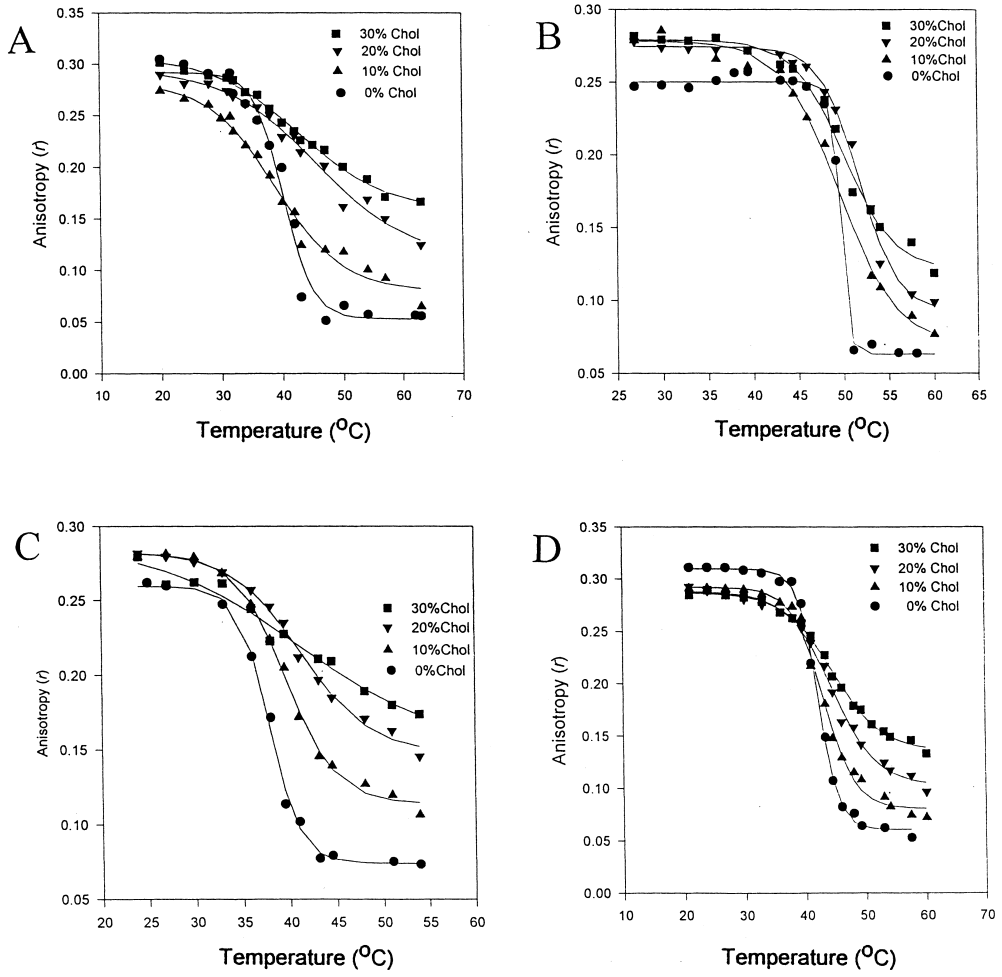

Fig. 1. Effect of cholesterol on the fluorescence anisotropy versus temperature plots of various lipid aggregates, (A) DODAB, (B) DOETAB, (C) DHPPC and (D) DPPC.

choline moiety at the headgroup level is replaced by an NMe_3^+ unit in **2**. Hence, DOETAB, **2**, is structurally related to both DODAB, **1**, and DPPC, **4**.

To examine the role of chain–backbone linkage function under the influence of a headgroup which is akin to naturally occurring DPPC, **4**, we also synthesized a phospholipid, DHPPC, **3**, which retains a PC residue at its headgroup. The PC residue in DHPPC at the headgroup level is separated from its lipophilic hydrocarbon chains by a similar distance as that in the DPPC backbone. However, the crucial difference between the structures of DHPPC and DPPC is in that the ester functionalities connecting the hydrophobic acyl chains in DPPC are missing in the former. Thus, the O-acyl linkage [O-C(=O)-] in DPPC has been replaced by two contiguous CH_2 units in DHPPC.

In the present study we compare the effect of cholesterol incorporation in membranes from each of the above lipids. These lipids form vesicles under identical conditions. TEM studies confirm the formation of vesicular aggregates from the new lipids **2** and **3** as well. Both of these aggregates contain inner aqueous compartments or they entrap solutes such riboflavin and CF, respectively.

3.2. *Steady-state fluorescence anisotropy measurements*

The anisotropies (r) were measured at different

temperatures and typical sigmoidal thermograms were observed with all lipid–cholesterol composite membranes (Fig. 1). Although the nature of the r versus T dependences was generally similar, the order parameters differed significantly from one plot to the other. The thermal phase transition parameters of the lipids and their cholesterol-doped membranes as determined from steady-state fluorescence spectroscopic studies of DPH are given in Table 1.

In the case of the naturally occurring phospholipid, DPPC, at 25°C, i.e. *below* the apparent gel-to-liquid-crystalline phase transition temperature (T_m), the r value *decreases* with the increase in the amount of cholesterol incorporated in the membrane (Fig. 1D). The decrease is somewhat pronounced upon cholesterol inclusion from 0 to 10 mol%. However, when cholesterol was included in excess of 10 mol%, the progressive decreases in the r values due to DPH in the mixed membrane were only modest. Thus, the incorporation of the cholesterol in DPPC membranes decreases the rigidity of the resulting bilayers below the T_m, which in other words suggests that the membranes become more fluid *below* the T_m.

With the lipids **1**, **2** and **3**, that do not contain ester type hydrocarbon chain–backbone connector function, the anisotropy as sensed by DPH, however, *increases* with the increase of the mol% of cholesterol in the gel phase of the membrane matrix (Fig. 1A–C). In the membranes composed of cationic lipids alone, the interaction between the lipid monomers should be considerably weaker than that in DPPC, due to unfavorable electrostatic repulsion at the level of their headgroup in membranes. Thus for the pure cationic lipid membranes the initial r values are considerably lower than that in DPPC bilayers. Acting as filler molecule, cholesterol reduces the inter-monomer lipid headgroup repulsion in these cationic lipid assemblies.

Interfacial hydration of the lipid bilayer aggregates is important for the maintenance of cell membrane architecture [47,48]. Such water molecules are presumed to participate in a hydrogen bonded network that extends between the constituent lipids of the membrane [49,50]. The headgroup hydration serves to optimize the hydrophobic effect by partially shielding the large coulombic repulsion between the charged headgroups.

Since, in the linker region of these lipids, **1**–**3**, there is no functional group that can associate with the water molecules via hydrogen bonding, water penetration does not significantly become enhanced at the Gouy–Chapman layers of these membranes. This

Table 1
Thermal phase transition parameters of the lipids and their cholesterol-doped membranes as determined by fluorescence spectroscopy[a]

Lipid	% Cholesterol	r (25°C)	T_m (°C)[b]	ΔT_m (K)[c]	r (T_m+10°C)
DODAB	0	0.29	42.2	9.0	0.15
	10	0.27	38.0	14.5	0.19
	20	0.28		d	0.24
	30	0.29		d	0.25
DOETAB	0	0.25	49.6	2.9	0.06
	10	0.28	49.6	11.6	0.08
	20	0.27		d	0.10
	30	0.28		d	0.13
DHPPC	0	0.26	37.4	6.7	0.07
	10	0.29	39.5	10.2	0.12
	20	0.28		d	0.16
	30	0.27		d	0.19
DPPC		0.31	42.2	6.9	0.06
	10	0.29	42.2	10.8	0.09
	20	0.29		d	0.12
	30	0.28		d	0.15

[a]See Section 2 for experimental methods.
[b]At least two preparations of vesicles were made from each lipid or lipid/cholesterol blends. The data presented are the averages of three measurements. The melting temperatures, T_m, are accurate to ±1°C.
[c]The ΔT_m values are accurate to ±2°C. d: clear breaks due to solid to fluid melting transition were blurred.

trend is not only valid for the cationic lipids of two different types, i.e. DODAB, **1**, and DOETAB, **2**, but also with the (C-1, C-2) dialkyl analog of the DPPC molecule, i.e. DHPPC, **3**. In the case of DHPPC, the intermolecular PC–PC headgroup level interactions are reduced on incorporation of cholesterol as happens for the DPPC membrane. However, the increase in the r values with the increase in cholesterol indicates that the linker region of DHPPC cannot retain as many water molecules as that in DPPC at the Gouy–Chapman layers. Then it should be the hydrophobic effect of cholesterol that plays the predominant role in the rigidification of the DHPPC membrane.

At temperatures 10°C above the T_m of the lipids, however, irrespective of their molecular structures, the r value increases remarkably with the increase in the concentration of cholesterol in the membrane. Up to 10 mol% of cholesterol incorporation, clear phase transition was observed for the mixed membranes in all cases. The sharpness of the phase transition process, however, was blurred with the incorporation of 20 mol% or more of cholesterol and the co-operativities of the thermal transitions were severely reduced. Notably, this scenario is not only observed for natural lipid DPPC, which contains ester linkages between hydrocarbon chains, and the glycerol backbone but is also observed with the lipids which do not have any ester type functional group connecting the hydrocarbon chain with the backbone bearing polar headgroups. Above the phase transition, the lipid organizations in membrane are highly disordered allowing enhanced hydration of the bilayer interface region. Since the r values increase with cholesterol above T_m, a more rigid environment is created with the increase in cholesterol concentration. As this finding is similar irrespective of the structure at the chain–backbone linkages, the hydrophobic effect of the cholesterol moiety must be primarily responsible for the dramatic increase in the order of the resulting lipid aggregates.

3.3. *Effect of cholesterol on the emission lifetime of vesicle-doped DPH*

To determine if water penetration is altered upon cholesterol inclusion in membranes, the lifetime of the excited state of the fluorophore DPH, which is located in the central region of the bilayer [51] was exploited. The value of the fluorescence lifetime yields information on the average environment of the fluorophore. The presence of water decreases this value due to the higher dielectric constant. In the present study we examined the lifetime of DPH embedded in a given lipid aggregate in the presence or in the absence of cholesterol at 25°C. The rate constants obtained in these experiments are of the same order as those measured in homogeneous solution, suggesting that a similar deactivation mechanism probably operates under these conditions. A typical decay profile of the excited DPH in cholesterol-doped DHPPC membrane is shown in Fig. 2 (inset). Examination of the decay curves of the vesicular solutions reveals the biphasic nature of these traces. From biexponential analysis it has been found that the minor phase (shorter lifetime) depends on the details of the method used in the sample preparation. However, the major component ($>90\%$) was found to depend on the cholesterol concentration. In Fig. 2, the τ/τ_{max} values are plotted against the cholesterol concentration. As is evident from Fig. 2 the τ/τ_{max} values increase in the case of *cationic* lipids with the

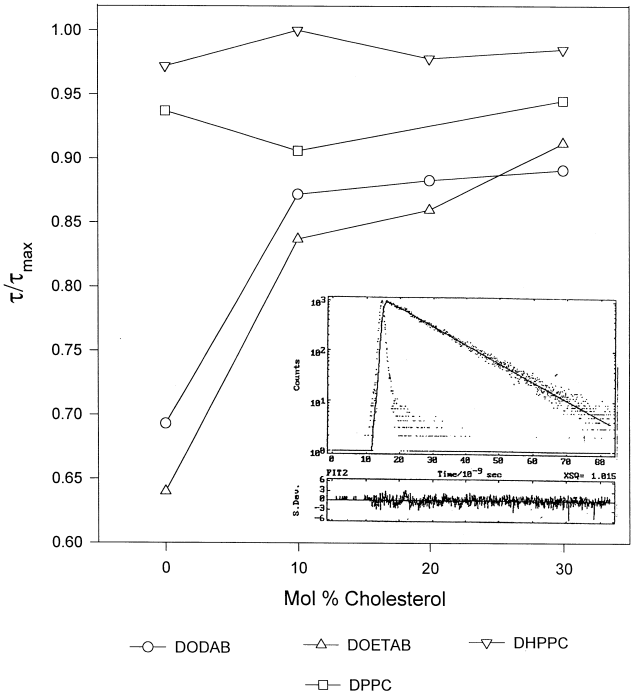

Fig. 2. τ/τ_{max} plot of DPH in cholesterol-free and laced lipid membranes. Inset: typical decay profile of the excited DPH in DHPPC membrane consisting of 20 mol% of cholesterol.

incorporation of cholesterol before reaching a plateau. On the other hand the changes of τ/τ_{max} as functions of cholesterol concentration are far less pronounced with *zwitterionic* PC lipids.

The progressive inclusion of cholesterol caused the fluorescence lifetime to increase from 8.6 to 11.1×10^{-9} s for DOTAB and from 7.9 to 11.3×10^{-9} s for DOETAB, as found with DPH. Thus, cholesterol addition reduces the water content of these cationic lipid bilayers. In the case of DHPPC, the lifetime value does not increase much with cholesterol incorporation. However, it is clear that DPH experiences a more hydrophobic environment in DHPPC to begin with, i.e. even in the absence of cholesterol, especially when one compares this against DODAB. Nevertheless, the DPH lifetime increases with the addition of cholesterol to a reduced extent. The higher r value suggests a more ordered packing arrangement at the hydrophobic part of the DHPPC membrane where DPH partitions. In the case of DPPC, the lifetime follows the same trend as is found in steady-state r values. It decreases slightly with an increase in cholesterol content. The reduction in stabilizing monomer–monomer interactions by incorporation of cholesterol might be responsible for the decrease in the lifetime values.

At room temperature (25°C), while the anisotropy values *decrease* in DPPC membranes with an *increase* in cholesterol concentration, the r value *increases* in the case of DOTAB and DHPPC. The increase in r values suggests the formation of a more ordered system. The fluidization of the DPPC matrix on incorporation of cholesterol might be explained by the fact that the 'filler' molecule, cholesterol, set the DPPC monomers apart in the membrane and 'dissociates' the interactions that might be present among DPPC monomers through hydrogen bonding at the ester linkages of the glycerol backbone. This 'loosening' of the inter-monomeric association between lipids reduces the packing arrangement upon inclusion of cholesterol.

In the cases of DOETAB and DHPPC, the absence of any linkage groups does not provide strong inter-monomeric stabilization as in the case of DPPC. Thus, they have much lower r values than that of DPPC. On incorporation of cholesterol in DOETAB membrane the DOETAB monomers become separated and the repulsive forces that prevail at the headgroup level decrease. In this situation the interfacial region of the membrane presumably becomes more hydrated due to the presence of the OH group of cholesterol. The reduction of the destabilizing force and the increase in hydration at the interface helps the DOETAB membrane to organize in a more ordered manner in the presence of cholesterol. Although in the case of DHPPC no headgroup level repulsive forces might be operative, the interfacial hydration should help the membrane matrix to organize in a better fashion upon incorporation of cholesterol. This explains why the order of the membrane matrix of DHPPC increases with the inclusion of cholesterol.

3.4. ^{1}H-NMR experiments

From the temperature-dependent fluorescence anisotropy measurements with different cholesterol-doped lipid assemblies, it was found that the perturbation induced by cholesterol in individual mixtures was less pronounced below their phase transition temperatures and the effect of cholesterol was more conspicuous above their T_m values. To obtain more information in the fluid state, the ^{1}H-NMR spectra of different lipid aggregates were examined at 60°C where they most likely remained in their fluid states. Fig. 3 shows the chain $(CH_2)_n$ and the terminal CH_3 resonance for each of the four lipids in the absence and in the presence of cholesterol. In all instances the addition of cholesterol in increments, from 0 to 30 mol%, led to a progressive broadening of the downfield $(CH_2)_n$ proton signals indicating that while cholesterol significantly restricted the mobility of the $(CH_2)_n$ units of lipid acyl or alkyl chains, it had an insignificant effect on the terminal methyl groups. In other words, cholesterol resists the flexing of methylene units of each of these lipids from the headgroup–chain connector region spanning the entire length of cholesterol in the fluid state. Therefore, the present findings illustrate that the 'immobilization' of $(CH_2)_n$ segments in lipid chains occur upon inclusion of cholesterol irrespective of the structure of the headgroup or its charge and the functional groups that link the backbone with the long hydrocarbon chains.

Fig. 4 shows the dependences of the ratio of the

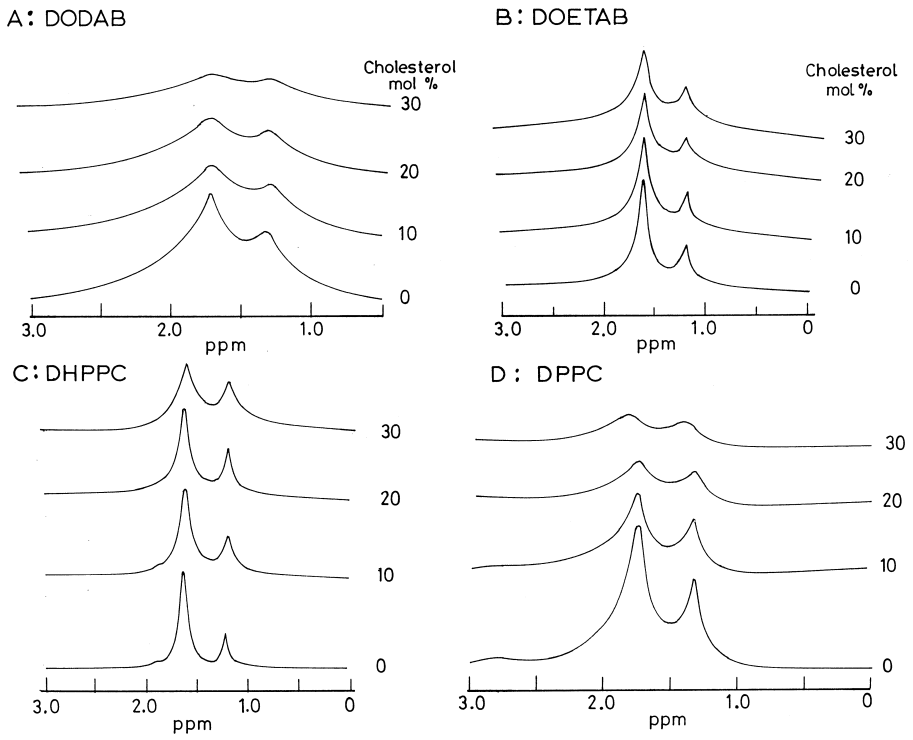

Fig. 3. Plots of ^{1}H-NMR signals of all the lipids at different concentrations of cholesterol.

widths at half-height of $(CH_2)_n$ to terminal CH_3 proton signals as a function of the incorporated cholesterol concentration. Generally the increase in cholesterol content caused an increase in the $\nu_{CH_2}^{1/2}/\nu_{CH_3}^{1/2}$ ratio for the cholesterol-doped vesicles. Upon addition of cholesterol, each lipid membrane behaved almost similarly, although the extent of variation of the ratio $\nu_{CH_2}^{1/2}/\nu_{CH_3}^{1/2}$ as a function of cholesterol concentration depended on the molecular structure of the host lipid. It is also apparent that the extent of motional restriction imparted by cholesterol depends on the lipid structure.

In general, for parent lipids alone, i.e. in the absence of cholesterol, the rotational relaxation time for the $(CH_2)_n$ unit is more for the cationic lipids than lipids containing a zwitterionic phosphocholine headgroup. This might be attributed to the increased translational motion of the cationic lipids due to the headgroup repulsion in these lipids, which makes the packing of lipids in the membranes looser. In the case of lipids with a zwitterionic phosphocholine headgroup, the translational lipid motion in membranes is expected to be lower due to their better monomer–monomer interactions especially in their hydrated conditions. The contribution of lipid–lipid hydrogen bonding interactions in PC lipids at the

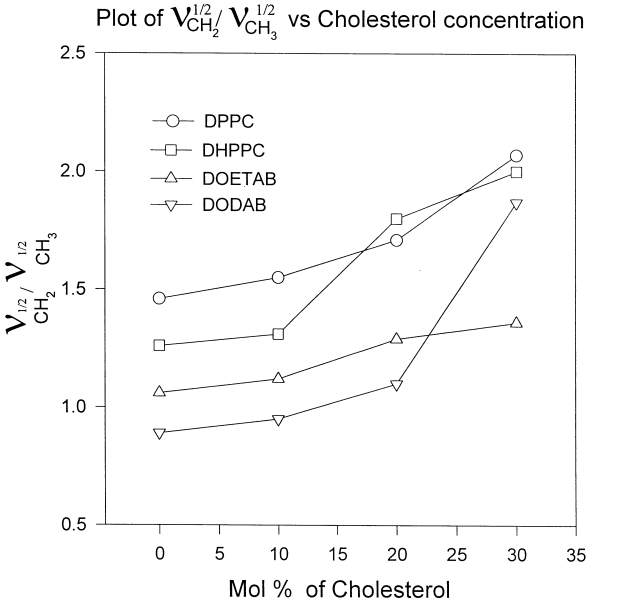

Fig. 4. The plots of the ratio of the widths at half height of polymethylene $(CH_2)_n$ to terminal methyl (CH_3) proton signals $(\nu_{CH_2}^{1/2}/\nu_{CH_3}^{1/2})$ against cholesterol concentration. (▽) DODAB, (△) DOETAB, (□) DHPPC, (○) DPPC.

hydration layer plays an important role in ordering the lipid assemblies in their membranes [52]. Since, cholesterol acts as a filler molecule and increases the monomer–monomer separation, inclusion of cholesterol into cationic lipid membranes mitigates headgroup repulsion between the lipid monomers. This is one reason why cholesterol inclusion improves restriction of the translational motion of cationic lipids in the resulting membranes and likewise mitigates the rotational relaxation of the $(CH_2)_n$ units. On incorporation of cholesterol, its rigid hydrophobic skeleton is placed in contact with the hydrophobic region of the cationic lipids and quenches the lipid hydrocarbon chain mobility due to the Van der Waals stabilization. The increase in the amount of cholesterol restricts the motional freedom of lipid monomers and the rotational relaxation time of the CH_2 units rather than the terminal CH_3 unit. As a result of this, the $\nu_{CH_2}^{1/2}/\nu_{CH_3}^{1/2}$ value increases with the increase in cholesterol content. The small difference that was observed between DODAB and DOETAB systems can be attributed to the differences in their molecular structures. While DODAB contains two hydrocarbon chains that are geminally, directly and symmetrically attached to the NMe_2^+ headgroup, DOETAB has its vicinally attached hydrocarbon chains separated from the NMe_3^+ headgroup by one CH_2 unit. Since, the ratio of $\nu_{CH_2}^{1/2}/\nu_{CH_3}^{1/2}$ gives a measurement of relative freedom of rotational relaxation of CH_2 units with respect to terminal CH_3, the tightness in the lipid can be estimated from this value. As the value of $\nu_{CH_2}^{1/2}/\nu_{CH_3}^{1/2}$ increases the alkyl chain packing in the membranes becomes tighter.

Therefore, for the cholesterol-free individual lipid membranes, the 'tightness' in lipid packing in membranous assemblies is minimal in the case of DODAB and increases to some extent for DOETAB presumably due to a separation of the cationic headgroup by one CH_2 unit from its hydrocarbon chains. In contrast, the lipids with a PC headgroup to begin with pack considerably better in membranes. The absence of significant inter-lipid repulsive forces at the headgroup level for the PC lipids makes these membranes tighter in organization. Indeed both phospholipid membranes show greater order. While the PC headgroup from either DHPPC or DPPC should interact with cholesterol in the same way, it is the difference in their functional group that attaches the hydrocarbon chains with lipid backbone which is probably responsible for the observed differences. Thus, the lipid packing in DPPC is further improved due to the presence of *ester* linkages with the hydrocarbon chains at the glycerol backbone. This improves lipid inter-monomer association possibly through better hydration and hydrogen bonding interactions with interfacially associated water molecules. DHPPC packs less effectively than DPPC as this hydrogen bonding might be absent in the former. On incorporation of cholesterol to each type of lipid suspension, the motion of $(CH_2)_n$ units in hydrocarbon chains becomes restricted and the $\nu_{CH_2}^{1/2}/\nu_{CH_3}^{1/2}$ ratios increase. This scenario is experienced with either type of lipid, but the extent varies to which they could be attributed to their architectural differences at the monomer level.

3.5. Dye entrapments

3.5.1. Efflux of CF from PC vesicles

In order to examine whether the incorporation of cholesterol influences the transmembrane permeation as a function of hydrocarbon chain–lipid backbone connector, we decided to entrap a probe (5/6-CF) in phospholipid vesicles. The ability to entrap a water-soluble dye in a vesicle implies that the vesicle is closed and that it contains an inner aqueous compartment. Since, in the MLVs, the dye might be trapped inside the inter-lamellar spaces, the unilamellar vesicles were prepared in the presence of CF.

It is important to note that in the present experiment we have chosen DMPC (dimyristoylphosphatidylcholine) instead of DPPC as the PC with diester links. This is due to the fact that even the pure DPPC vesicles ($T_m \sim 42°C$) are very resistant to CF release at 25°C and cholesterol incorporation leads to a further reduction in its CF-efflux rates. On the other hand, DMPC vesicles, in spite of having ester type linkages, are considerably more leaky at 25°C due to its lower phase transition temperature ($T_m \sim 24°C$). Therefore, the relative reduction in the CF efflux rates upon cholesterol incorporation is more pronounced with DMPC than with DPPC at 25°C.

The two phospholipids chosen for this study were identical except that while DMPC has ester type (O-C=O) linkages between the hydrocarbon chain and

glycerol backbone of the lipid, the two alkyl chains in DHPPC are linked through CH_2–CH_2 residues. Therefore, if the interaction of cholesterol through its 3β-OH group with the –C=O groups of the ester linkages of the hydrocarbon chains of phospholipids plays a role in controlling the permeability, then the efflux rates of the entrapped dye CF would be significantly different between the membranes of DMPC and DHPPC as a function of cholesterol concentration. The other lipids with a cationic headgroup could not be used in this study as CF adhered with cationic interfaces due to the anionic character of CF.

The time-dependent enhancement of the fluorescence emission of CF was taken as a direct measure of the CF efflux rates from vesicles. A histogram showing the effect of incorporation of cholesterol on the release of entrapped CF from vesicular DHPPC and DMPC is shown in Fig. 5. From the results obtained on the time-dependent CF release experiment at 25°C, it is clear that cholesterol modulates the permeability properties of the membrane remarkably and the efflux rate of CF from the membrane decreased significantly with the increase in the amount of cholesterol incorporated in the bilayer matrix of either type of phospholipid vesicles. Strikingly the effect of cholesterol inclusion on the efflux rates of CF was not different irrespective of the nature of the chain–headgroup connector functional groups. For DMPC, at 25°C, the vesicles ($T_m \sim 24$°C) are already in their fluid state. The intrinsic efflux rates of CF from fluid DMPC vesicles were therefore higher than the corresponding rates from DHPPC vesicles ($T_m \sim 37$°C) as the latter remain in their rigid gel-like states at 25°C. These findings clearly demonstrate that the presence of cholesterol seems to reduce the bilayer permeability similarly from the lipid with either type of chain–backbone linkage. This implies that the ability or inability of a lipid to associate with the 3β-OH group of cholesterol via its hydrocarbon–backbone linkage functional group does not influence the permeation of an entrapped dye from the respective membranes.

3.5.2. *Dye entrapment in cationic lipid vesicles and trans-membrane permeation assay*

The entrapment of a neutral dye, riboflavin, in either the cationic lipid vesicles of DODAB, **1**, or DOETAB, **2**, was performed following a published procedure [4].

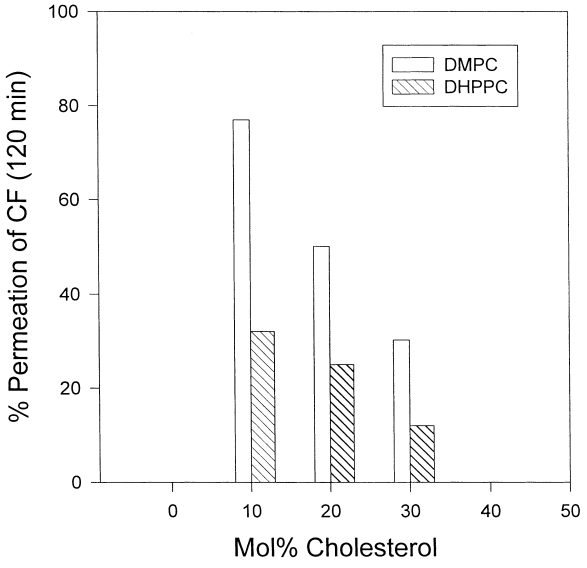

Fig. 5. A bar plot of the percentage CF leakage after 120 min of incubation at 25°C with vesicular DMPC and DHPPC in the presence of cholesterol. Note that for the aggregate devoid of cholesterol, the leakage was considered to be 100%.

The fluorescence intensity of vesicle-bound riboflavin was measured at ~514 nm with an excitation wavelength of 375 nm. This included the dye molecules entrapped within the inner pools of the vesicles in addition to the riboflavin adsorbed on the vesicle surfaces. As the pH of the sample was raised from 6.4 to ~10.2 at 25°C, the emission at 514 nm decreased rapidly to 60±3% of the original fluorescence intensity recorded prior to pH adjustment. The residual fluorescence quenched in a time-dependent fashion following a single exponential decay. From the decay traces, the pseudo-first-order rate constants could be obtained. We attribute the rapid fluorescence loss (~40%) due to the deprotonation of the riboflavin molecules adhering at the outer vesicle surfaces and the time-dependent phase due to the trans-membrane permeation of OH^- ions across the vesicles under the imposed pH gradient. These rates differed with the amount of cholesterol included in a given cationic lipid vesicle and allowed examination of the effect of cholesterol inclusion on the trans-membrane permeation rates.

We compared the half times of this time-dependent process for different vesicles with or without cholesterol. At 25°C, i.e. $< T_m$, the riboflavin loaded cat-

ionic vesicular suspensions were all in their rigid, less permeable gel phases. Although the differences in permeability among various vesicular blends that were examined are not very large, they are significant. It appears that the vesicles with the dialkyl type geminal hydrophobic architecture such as in **1** are more leaky than their vicinal counterparts, **2**. In spite of these intrinsic differences, the permeation rates of OH^- ions across the vesicles under the imposed pH gradient were appreciably reduced with either type of cationic lipid upon incorporation of cholesterol in their covesicular aggregates. Thus, while the half time for OH^- ion permeation for vesicular **1** is $\sim$7.6 min, the corresponding values for the coaggregates of **1** doped with 10 and 20% cholesterol were $\sim$10.2 and $\sim$13.3 min, respectively. Similarly while the half-time for OH^- ion permeation for vesicular **2** is $\sim$10.3 min, the corresponding values for the coaggregates of **2** doped with 10 and 20% cholesterol were $\sim$14.3 and $\sim$16 min, respectively. Clearly the incorporation of cholesterol into either type of cationic lipid vesicles reduced the rates of OH^- ion permeation irrespective of the molecular structures of the lipids. It is noteworthy that there is no possibility for hydrogen bond formation at the 3β-OH of the cholesterol molecule with any of these cationic lipids either at the level of headgroup or at their chain–backbone connections.

3.6. X-ray diffraction of cast films of lipids

To obtain insight on the effect of cholesterol incorporation on the bilayer thicknesses of various lipid suspensions, X-ray diffractions of the cast films from aqueous suspensions of various lipids and their different cholesterol-doped samples were examined. It is assumed that upon casting, the bilayer or multi-layer vesicles collapse and form 'stacked' lamellar layers [38,39]. Periodic peaks in small and middle angle diffraction from cast films on glass plates could be attributed to the reflection from planes of the multiple lamellar structure. The spacing of higher order reflections ($h>1$) is satisfied with a numerical relation of $1/h$ of the long period calculated from the first-order reflection, which is equivalent to the thickness or width of the bilayer.

The variations in the bilayer thicknesses upon incorporation of cholesterol in various lipid membranes are shown in Fig. 6. In the case of DPPC, the bilayer thickness first increased from 55.7 to 58.9 Å on incorporation of 10 mol% cholesterol. Further cholesterol inclusion caused a progressive reduction in bilayer thickness of the resulting membranes. The decreasing trends in these bilayer thicknesses were also observed with the membranes from other two lipid systems, such as DOETAB and DHPPC, upon incorporation of cholesterol in their bilayer matrix.

Earlier investigations report that the incorporation of cholesterol induces a reduction in the membrane thicknesses of the membranes containing lecithin [53,54]. Therefore, the present observations are in agreement with the literature. Since in the present study, reflection patterns characteristic of lamellar organizations were observed in each case, the decreases in the membrane thicknesses might be attributed to the increase in the tilt angle of the lipid molecules with respect to the bilayer normal upon incorporation of cholesterol (Table 2). These could be presumably due to lateral reorganization of the hydrophobic core of membranes upon inclusion of cholesterol, which induces greater monomer separation in the cholesterol-laced membranes. This again shows that irrespective of whether the hydrogen bonding interaction between 3β-OH of cholesterol

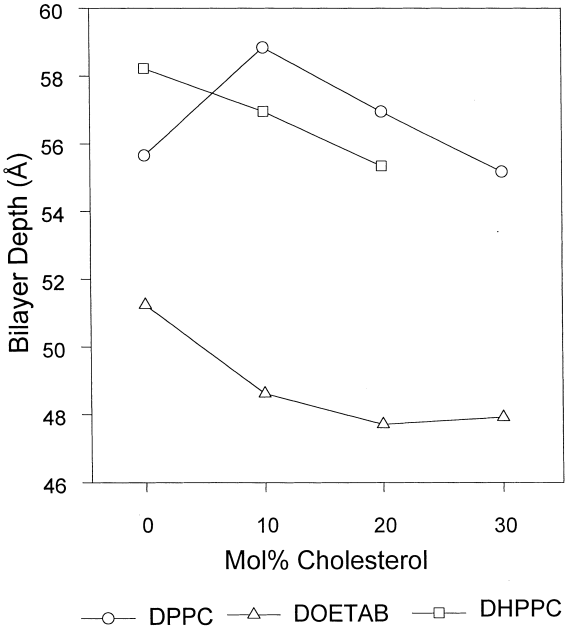

Fig. 6. First order reflections of XRD versus cholesterol concentration (doped amphiphilic systems).

and the functional groups that link the hydrocarbon chains with the lipid backbone is present or not, the effects on the bilayer thicknesses upon inclusion of cholesterol are similar. The origin of cholesterol induced reduction in bilayer widths should therefore be hydrophobic and does not depend on the nature of the chain–backbone linkages of the lipid.

3.7. Conclusions

These observations indicate that the action of cholesterol in generating the ordered environment in PC or cationic lipid model membranes is quite general and do not depend on the lipid headgroup structure or charge and the nature of chain–backbone links. The contribution of the hydrogen bonding to the overall inter-lipid interaction is influenced by headgroup charges and, therefore, in a situation (cationic lipid) where the headgroup repulsion is high to begin with, cholesterol incorporation increases the headgroup spacing and stabilizes the resulting bilayer membranes. Hydrophobic stabilization of the mixed bilayer is then reinforced via quenching of the chain motion by the incorporation of a cholesterol molecule. The decreases in CF permeability generated by cholesterol incorporation occurred independently of the presence of a linkage functional group in the PC lipids which may participate in the hydrogen-bonding interaction with the 3β-OH of cholesterol. Similarly, a reduction in the rates of OH^- ion permeation based on fluorescence quenching of the vesicle entrapped riboflavin suggests that even in the case of cationic lipids, cholesterol causes similar effects to those seen with PC lipids. In this instance with cationic lipids, a hydrogen-bonding interaction is not possible either at the headgroup or at the chain–backbone links. Taken together this suggests that the observed cholesterol induced effects are brought about by an increase in the Van der Waals interactions between adjacent lipid hydrocarbon chains induced by the condensing effects of cholesterol. It is therefore clear that the presence of hydrogen bonding either between the lipid linkage region or the headgroup and the 3β-OH of cholesterol is not necessary to explain the observed cholesterol induced effects in membranes.

Table 2
Bilayer thickness of the cholesterol-free and cholesterol-laced lipid membranes, measured by cast film X-ray diffraction

Lipid	% Cholesterol	Bilayer width	Tilt angle[a]
DOETAB	0	51.2	30.0
	10	48.6	34.8
	20	47.7	36.3
	30	47.9	36.0
DHPPC	0	58.2	23.8
	10	57.0	26.5
	20	55.3	29.6
	30	57.9	26.5
DPPC	0	55.7	25.0
	10	58.9	16.6
	20	57.0	21.9
	30	55.2	26.0

[a]Tilt angle (α): the disposition of the long axis of the lipid molecule to the normal of the lipid bilayer surface as estimated from the equation $\alpha = \cos^{-1}(L_x/L_c)$, where L_x is the bilayer depth obtained from the XRD measurement and L_c is the length of the bilayer calculated from molecular modeling studies.

Acknowledgements

This work was supported by a Swarnajayanti Fellowship grant from the Department of Science and Technology, Government of India. We thank Dr. B. Maiya of the University of Hydraobad for giving access to IBH-500 single photon counting instrument.

References

[1] K. Block, in: D.E. Vance, J.E. Vance (Eds.), Biochemistry of Lipids and Membranes, Benjamin/Cummins, Menlo Park, CA, 1985.
[2] P.L. Yeagle, Biochim. Biophys. Acta 822 (1985) 267.
[3] C. Vichèze, T.P.W. McMullen, R.N. McElhaney, R. Bittmann, Biochim. Biophys. Acta 1279 (1996) 235.
[4] R.A. Demel, L.L. van Deenen, B.A. Pethica, Biochim. Biophys. Acta 135 (1967) 11.
[5] P. Joose, R.A. Demel, Biochim. Biophys. Acta 183 (1969) 447.
[6] S.F. Bush, I.W. Levin, Chem. Phys. Lipids 27 (1980) 101.
[7] S. Clejan, R. Bittman, P.W. Deroo, Y.A. Isaacson, A.F. Rosenthal, Biochemistry 18 (1979) 2118.
[8] R.A. Demel, Biochim. Biophys. Acta 457 (1976) 109.
[9] J.L.R. Rubenstein, B.A. Smith, H.M. McConnell, Proc. Natl. Acad. Sci. USA 76 (1979) 15.
[10] A.-L. Kuo, C.G. Wade, Biochemistry 18 (1979) 2300.
[11] R. Semer, E. Gelerinter, Chem. Phys. Lipids 23 (1973) 201.

[12] M.-P. Gierula, W.K. Subczynski, K. Kusumi, Biochemistry 29 (1990) 4059.
[13] W.L. Hubbel, H.M. McConnell, J. Am. Chem. Soc. 93 (1971) 314.
[14] M. Delmelle, K.W. Butler, I.C.P. Smith, Biochemistry 19 (1980) 698.
[15] J.L. Lippert, W.L. Peticolas, Proc. Natl. Acad. Sci. USA 68 (1971) 1572.
[16] R. Mendelson, Biochim. Biophys. Acta 290 (1972) 15.
[17] J. Umemura, D.G. Cameron, H.H. Mantach, Biochim. Biophys. Acta 602 (1980) 32.
[18] G.W. Stockton, C.F. Polnaszek, A.P. Tulloch, F. Hassan, I.C.P. Smith, Biochemistry 15 (1976) 954.
[19] S.P. Verma, D.F.H. Wallach, Biochim. Biophys. Acta 330 (1973) 122.
[20] P.L. Yeagle, R.B. Marlin, Biophys. Biochem. Res. Commun. 69 (1976) 775.
[21] N.P. Franks, W.R. Lieb, J. Mol. Biol. 133 (1979) 469.
[22] C.-H. Huang, Lipids 12 (1977) 348.
[23] E. Bicknell-Brown, K.G. Brown, Biophys. Biochem. Res. Commun. 94 (1980) 638.
[24] S.F. Bush, R.G. Adams, I.W. Levin, Biochemistry 19 (1980) 4429.
[25] R. Bitmann, S. Clejan, S. Lund-katz, M.C. Phillips, Biochim. Biophys. Acta 772 (1984) 117.
[26] R.A. Demel, A.K. Lala, S. Nanda Kumari, L.L.M. van Deenen, Biochim. Biophys. Acta 771 (1984) 142.
[27] C. Karolis, H.G.L. Coster, C.T. Chilcott, K.D. Barrow, Biochim. Biophys. Acta 1368 (1998) 247.
[28] S. Bhattacharya, S. Haldar, Biochim. Biophys. Acta 1283 (1996) 21.
[29] S. Bhattacharya, S. De, M. Subramanian, J. Org. Chem. 63 (1998) 7140.
[30] S. Bhattacharya, S. De, S.K. George, Chem. Commun. (1997) 2287.
[31] S. Bhattacharya, S.S. Mandal, Biochim. Biophys. Acta 1323 (1997) 29.
[32] S. Bhattacharya, S. Ghosh, K.R.K. Easwaran, J. Org. Chem. 63 (1998) 9232.
[33] S. Haldar, Ph.D. Thesis, Indian Institute of Science, Bangalore, 1999.
[34] J. Lakowicz, Principles of Fluorescence Spectroscopy, Plenum Press, New York, 1983, p. 44.
[35] M. Shinitzky, Y. Barenholtz, Biochim. Biophys. Acta 525 (1978) 367.
[36] M. Shinitzky, M. Inber, Biochim. Biophys. Acta 433 (1976) 133.
[37] H. Pottel, W.V.D. Meer, W. Herreman, Biochim. Biophys. Acta 730 (1983) 181.
[38] J.N. Winstein, S. Yoshikami, P. Henkart, R. Blumenthal, W.A. Hagins, Science 195 (1977) 489.
[39] R. Neumann, H. Ringsdorf, E.V. Patton, D.F. O'Brien, Biochim. Biophys. Acta 898 (1987) 338.
[40] S. Bhattacharya, S. Haldar, Langmuir 11 (1995) 4748.
[41] Y. Wakayama, T. Kunitake, Chem. Lett. (1983) 1425.
[42] N. Kimizuka, T. Kawasaki, T. Kunitake, J. Am. Chem. Soc. 115 (1993) 4328.
[43] J.M. Boggs, Biochem. Cell. Biol. 64 (1986) 50.
[44] S.J. Friedberg, M. Holpert, J. Lipid Res. 19 (1978) 57.
[45] R. Bittman, S. Clejan, M.K. Jain, P.W. Deroo, A.F. Rosenthal, Biochemistry 20 (1981) 2790.
[46] J. Seelig, A. Seelig, Q. Rev. Biophys. 13 (1980) 19.
[47] J.M. Boggs, Biochim. Biophys. Acta 906 (1987) 352.
[48] H. Brokerhoff, Lipids 17 (1982) 1001.
[49] M. Prats, J.F. Tocanne, J. Teissic, Eur. J. Biochem. 1623 (1987) 79.
[50] J. Teissic, M. Prats, A. LeMassu, L.C. Stewart, M. Kates, Biochemistry 29 (1990) 59.
[51] L. Davanport, R.E. Daly, R.-H. Bisby, R.B. Cundall, Biochemistry 24 (1985) 4097.
[52] S.J. Slater, C. Ho, F.J. Taddeo, M.B. Kelly, C.D. Stubbs, Biochemistry 32 (1993) 3714.
[53] R.G. Ashcroft, H.G.L. Coster, J.R. Smith, Nature 269 (1977) 819.
[54] G.L. Turner, E. Oldfield, Nature 277 (1979) 669.